Xian *et al. Heritage Science* (2023) 11:236
https://doi.org/10.1186/s40494-023-01080-6

Heritage Science

RESEARCH Open Access

A method to characterize turquoise deposits in china using sedimentary environment sensitive elements

Yiheng Xian[1], Yun Liang[1], Chun Yu[1], Liping Yang[1] and Yanwang Wu[2*]

Abstract

'Fingerprint' identification is the key to turquoise provenance studies, but previous studies have met with limited success in China. Turquoises in China mainly occur in altered sedimentary rocks and are formed by weathering, leaching and sedimentation. This paper evaluates the potential for sedimentary environment sensitive elements to be used to distinguish between turquoise deposits in China. In this paper, the ratios of V/Mo, Ce/Ce*, Ni/Co, Sr/Ba, Tl/Ga, Li/Ba and V/Cr were calculated for turquoise of different origins. Our results show that these parameters when used alongside Ga concentration permit effective discrimination between turquoise sources in China. This approach brings to light a new means of analyzing trace element databases and an untapped wealth of information that can be used for future turquoise provenance studies.

Keywords Turquoise, Sedimentary environment sensitive elements, Provenance studies

Introduction

Turquoise has been used to make pendants, beads and inlay material in China since as early as c. 8600–9000 BP [1]. A remarkable number of turquoise artifacts have been discovered across a large number Late Neolithic and Bronze—Iron Age archaeological sites, suggesting that the acquisition and exchange of turquoise was an important aspect of these cultures. The procurement of turquoise and its use as a decorative material has previously been taken to reflect the economic, organizational, and social structure of the ancient cultures involved [2, 3].

Turquoise is a hydrated copper and aluminum phosphate with the chemical formula $A_{0\text{-}1}B_6(PO_4)_{4\text{-}x}(PO_4)_x(OH)_8 4H_2O$. When $X=0$, it is turquoise. The most common ion occupying the A position is Cu^{2+}, Fe^{2+}, Zn^{2+} or vacancy, and the B position is Fe^{3+} or Al^{3+} [4]. Turquoise produced in nature contains different impurity elements, and its composition content will deviate from the theoretical value. In order to understand the acquisition and exchange of turquoise among pre-historical societies, a reliable, quantitative method for linking turquoise artifacts to their geological sources is needed. Although the analysis of Pb and Sr isotopes has been used to successfully traces turquoise sources and networks in the southwestern United States and northern Mexico [5–7], but this technique has not satisfactorily differentiated among turquoise deposits in China. Hull et al. [8–10] used the isotope ratio of hydrogen and copper to characterize turquoise deposits in the United States and Mexico. The experimental results found that the hydrogen and copper isotopic characteristics of turquoise can distinguish turquoise from different origins. Recent study [11] used copper isotopes to distinguish between 11 samples of turquoise from three deposits in Hubei Province. Although this method initially offered considerable promise, no

---

*Correspondence:
Yanwang Wu
wuyanwang@126.com
[1] Key Laboratory of Cultural Heritage Research and Protection Technology, Ministry of Education, Northwest University, Xi'an 710069, People's Republic of China
[2] School of Geology and Geomatics, Tianjin Chengjian University, Tianjin 300384, People's Republic of China

further studies using this method have been published in China. Further studies [12] which attempted to characterize turquoise sources using Pb and Sr isotopic ratios proved unsatisfactory.

The utility of different geochemical techniques for lithic characterization is dependent on geochemical processes in effect during the formation of the mineral or rock that lead to detectable, source-specific variations in their material chemistry [13]. Compared to isotope analysis, trace element analysis can provide a more detailed almost 'genetic' profile for individual deposits. Therefore, trace-element analysis has, to date, remained the dominant approach through which to characterize and distinguish between turquoise sources in China [14–16]. However, most investigations to date have been done on a small scale, and at least one was unable to differentiate deposits based on trace-element profiles. In each case different trace elements were used to build the source signatures. Part of the problems arises from the fact that each of these papers has employed multiple techniques, including X-ray fluorescence, X-ray diffraction, laser denudation inductively coupled plasma spectrometry (LA-ICP-AES) and inductively coupled plasma mass spectrometry (ICP-MS). In addition, most investigators used a wide variety of statistical methods to identify differences in the trace element concentrations within each of the turquoise sources. In each case these methods failed to take the geological setting of the deposits into consideration.

This paper attempts to synthesize the extant geological and geochemical knowledge of turquoise deposits in China. Based on geological setting of the deposits, we reevaluate the functionality of trace element measurement as a means through which to distinguish between different turquoise deposits in China.

Geological setting and genesis

Turquoise deposits are broadly distributed across northern China with known historical sources in Anhui, Henan, Hubei, Shaanxi and Xinjiang provinces in China. The mineralization typically occurs as veins and nodules in altered sedimentary and igneous rocks, which have different ages and tectonic settings. Based on their geological settings, the occurrence of these deposits can be divided into three mineralization zones: Maanshan, Qinling and Hami (Fig. 1) [17].

In Qinling mineralization zone, turquoise is generally associated with Lower Cambrian black rock series, which mainly consists of siliceous, carbonaceous–siliceous slate, phyllite and schist [17]. Turquoise usually co-exists with carbonaceous material, limonite ($FeO(OH)\cdot H_2O$), secondary quartz (SiO_2), kaolinite ($Al_4[Si_4O_{10}](OH)_8$), allophane ($xSiO_2\cdot Al_2O_3\cdot yH_2O$) and other clay minerals [17]. Ancient turquoise mining ruins have been discovered in Baihe and Luonan, Shaanxi. Ancient mining caves, pottery shards, mining stone tools, turquoise minerals, etc. were found in the ruins. The ancient turquoise mining ruin in Luonan is the earliest turquoise mining

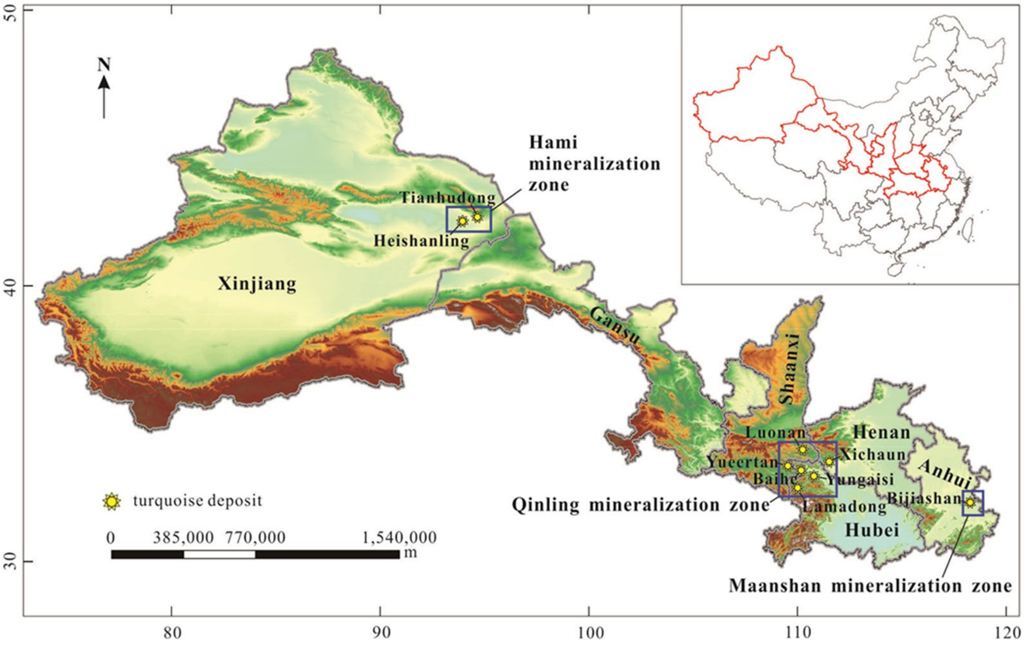

Fig. 1 Map showing the locations of the turquoise deposits in the Qinling, Hami and Maanshan mineralization zones

site discovered so far, ranging from 1900 to 500 BC [12]. Only preliminary archaeological research has been carried out on the ancient turquoise mining ruin in Baihe.

Similarly, turquoise in Hami mineralization zone is also associated with altered sedimentary rocks. The Heishanling and Tianhudong turquoise deposits both occur in the Lower Cambrian Shuangyingshan Formation, which mainly consists of foliated lithic sandstone, siliceous and marble, indicating that its sedimentation occurred in a shallow marine environment [18]. The mineralization usually associated with these rock types are usually limonite, quartz, sericite $((K,H_3O)(Al,Fe,Mg)_2(Si,Al)_4O_{10}[(OH)_2 \cdot H_2O)])$ and calcite ($CaCO_3$). Ancient turquoise mining ruins have also been discovered at Heishanling and Tianhudong. Ancient mining pits, pottery sherds, mining stone tools, house sites, processed turquoise, etc. were found in the ruins. According to the ^{14}C dating results, the age of the two ancient turquoise mining ruins is between 1300 and 400 BC [19].

Turquoise deposits in the Maanshan mineralization zone have an unusual context. Turquoise is principally found as veins and nodules in Early Cretaceous igneous complexes that are spatially and temporally associated with iron mineralization. These igneous rocks are mostly diorite porphyrite and andesite. The turquoise usually co-exists with kaolinite, pyrophyllite ($Al_2\ [Si_4O_{10}](OH)_2$), quartz, sericite, alunite ($KAl_3(SO_4)_2(OH)_6$), pyrite (FeS_2), opal ($SiO_2 \cdot nH_2O$), jarosite ($KFe_3(SO_4)_2(OH)_6$) and some anhydrite ($CaSO_4$), vivianite ($Fe_3(PO_4)_2 \cdot 8H_2O$) and wavellite ($Al_3(PO_4)_2(OH,F)_3 \cdot 5H_2O$) [20]. No ancient turquoise mining ruins have yet been discovered in this area.

Turquoise is generally formed by meteoric water flowing downward through host rocks, leaching elements and thereafter depositing in lower rock layers [21, 22], this means that it derives its elemental constituents from the surrounding geological formations. As mentioned above, Chinese turquoise occurs in altered sedimentary rocks which have formed under a variety of sedimentary environments, which lead to different redox conditions and salinity. This means that the turquoises have formed the weathering of rocks which contain a wide range of redox and salinity sensitive elements. In those previous studies in which variations in trace element signatures were recorded, redox and salinity sensitive elements V, Ni, Sr, Ba were also present [14–16]. This means that redox and salinity sensitive elements can used to differentiate Chinese turquoise deposits.

Trace element geochemistry

This paper presents 81 trace element analyses from 9 deposits, these samples were analyzed using inductively coupled plasma-mass spectrometry (ICP-MS). Most of these data are from the authors' group, and a few are from other scholars [14, 23]. Samples from the four sites of Baihe, Luonan, Heishanling, Tianhudong were from the ancient turquoise mining ruins.

Qinling mineralization zone

This zone can be further sub-divided into three smaller zones, south, middle and north, each of which shows distinct variations in the occurrence of REEs. Turquoise deposits in the south zone have varying rare earth elements (REE) concentrations (Table 1). They are all depleted in the most incompatible light-REE (LREE), while LREE is enriched in one sample from the Lamadong turquoise deposit (Fig. 2), and they exhibit obviously negative Ce and no obvious Eu anomalies (Table 1, Fig. 2). More detail ratios are shown in Table 1. The V, Cr, Mo, Ba, Cd, In, Zn and Cu concentrations in these turquoises are mostly higher than the upper continental crust (UCC), but the percentages of Li, Ni, Co, Sr, Tl, Pb, W, Th, Zr and Hf are lower than the UCC. Ga in Yueertan, Baihe and Lamadong turquoise deposits is close to

Table 1 Ratios of rare earth elements of turquoise in Qinling, Hami and Maanshan zone in China

Mineralization zone	**Qinling**						**Hami**		**Maanshan**
	South zone				**Middle zone**	**North zone**			
Deposit	**Yungaisi**	**Lamadong**	**Baihe**	**Yueertan**	**Xichuan**	**Luonan**	**Heishanling**	**Tianhudong**	**Bijiashan**
∑REE + Y (ppm)	14.09–289.72	9.57–328.73	7.22–154.92	7.44–16.75	15.82–599.07	5.69–21.46	3.11–212.33	4.42–158.42	2.62–102.04
$(La/Yb)_{UC}$	0.05–0.88	0.05–2.94	0.02–0.39	0.03–0.22	0.03–1.08	0.14–0.45	0.05–3.65	0.02–2.94	0.17–17.74
$(La/Sm)_{UC}$	0.03–0.31	0.12–0.62	0.06–0.32	0.20–0.26	0.08–0.50	0.09–0.20	0.11–1.24	0.04–0.74	0.26–2.89
$(Gd/Lu)_{UC}$	0.65–4.20	0.42–4.47	0.56–1.75	0.42–1.31	0.62–4.96	2.05–2.76	0.86–8.75	0.60–4.89	0.74–7.27
$(Ce/Ce^*)_{UC}$	0.30–0.74	0.30–0.46	0.52–0.73	0.64–0.66	0.30–0.53	0.54–0.71	0.61–0.90	0.54–0.70	0.87–0.99
$(Ce/Ce^*)_{CN}$	0.34–0.81	0.33–0.53	0.60–0.81	0.71–0.72	0.34–0.56	0.60–0.79	0.67–0.89	0.62–0.75	0.86–0.95
$(Eu/Eu^*)_{UC}$	1.06–1.21	0.87–1.03	0.91–1.48	0.85–1.22	0.59–1.32	1.02–1.06	0.63–3.75	0.91–3.47	0.62–1.94

Most of these data are from the authors' group, and a few are from other scholars [14, 23]

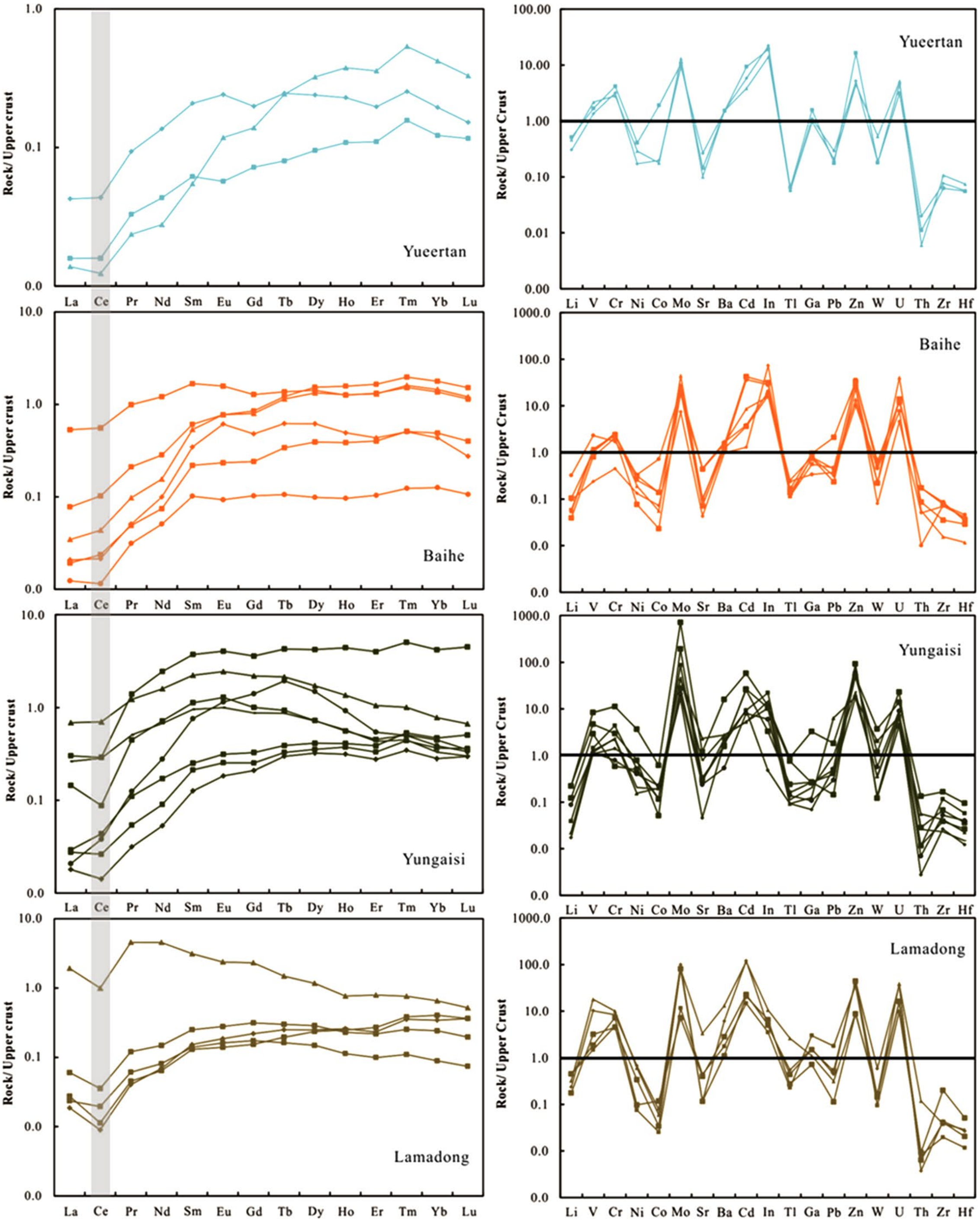

Fig. 2 Upper crust-normalized REE (right) and spider (left) diagrams for Yueertan, Baihe, Yungaisi and Lamadong turquoises in Qinling mineralization zone (Data normalizing values following Rundnick and Gao [24, 41])

the UCC, while the Yungaisi turquoise deposits have lower Ga concentrations than the UCC (Fig. 2).

Turquoise deposits in the middle zone, namely the Xichuan turquoise deposits, have higher REE concentrations (15.82–599.07 ppm) than those in the south zone. They are mostly depleted in LREE [$(La/Yb)_{UC}=0.03–1.08$], and show obviously negative Ce anomalies [$(Ce/Ce^{*})_{UC}=0.30–0.53$] (Table 1, Fig. 3).

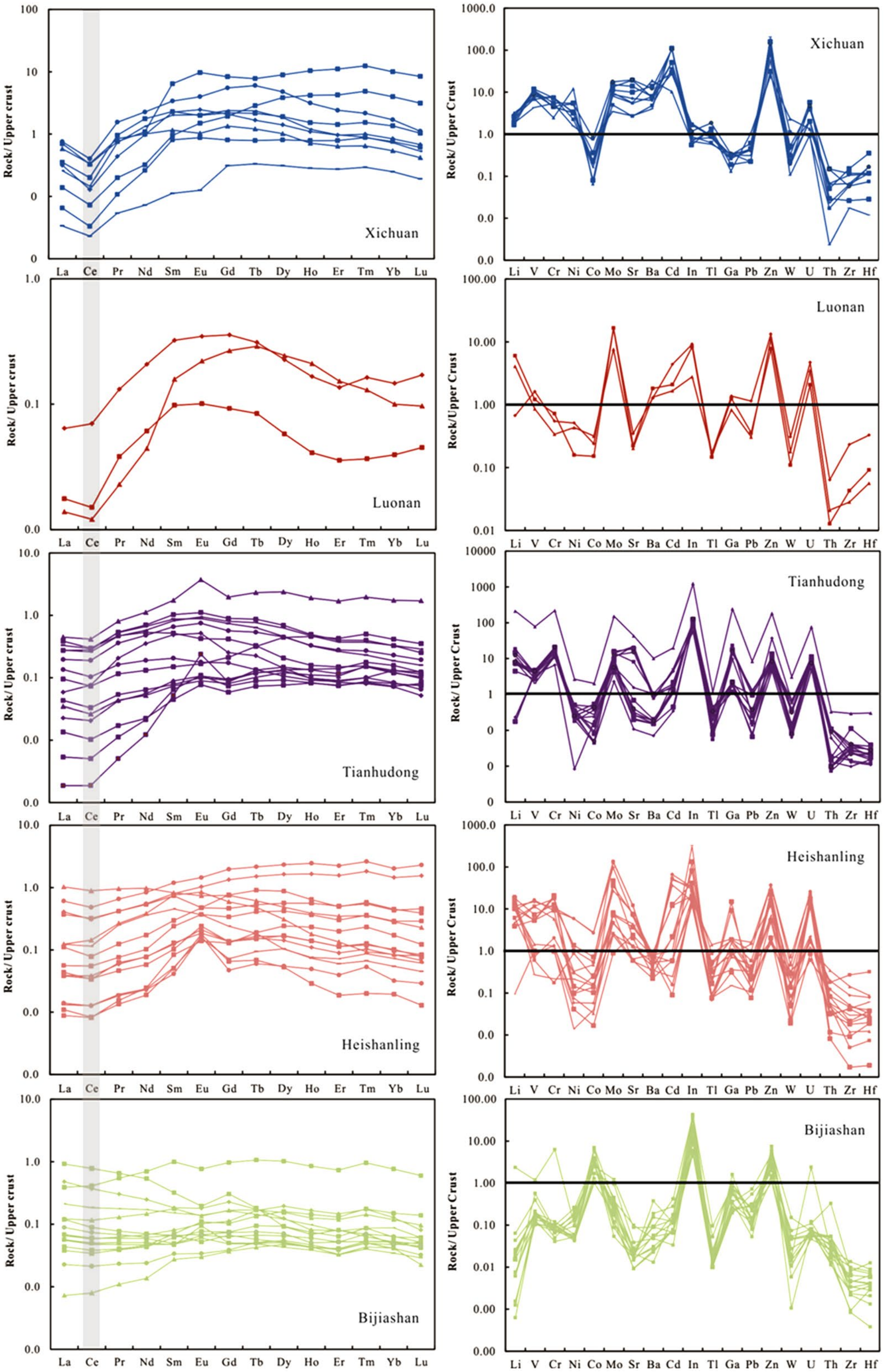

Fig. 3 Upper crust-normalized REE (right) and spider (left) diagrams for Xichuan and Luonan turquoises in Qinling mineralization zone, Tianhudong and Heishanling turquoises in Hami mineralization zone and Bijiashan turquoise in Maanshan mineralization zone (Data normalizing values following Rundnick and Gao [24, 41])

Compared with the UCC, the Xichuan turquoise deposits are enriched in Li, V, Cr, Ni, Mo, Sr, Ba, Ga, Zn and Cu, depleted in Co, Ga, Pb, W, Th, Zr and Hf (Fig. 3).

Turquoise deposits in the north zone, represented by the Luonan turquoise deposits, have low (REE) concentrations ranging from 5.69 to 21.46 ppm, similar to those seen in the Yueertan turquoise deposits. In comparison with the upper continental crust (UCC), they are enrichment in medium-REE (MREE, $(La/Sm)uc = 0.09–0.20 < 1$, $(Gd/Lu)uc = 2.05–2.76 > 1$), and depleted in Ce [$(Ce/Ce^*)_{UC} = 0.54–0.71$] (Table 1, Fig. 3). Luonan turquoises have higher concentrations of Li, Mo, Ba, Cd, In, Zn and Cu than those of the UCC, but depleted in Cr, Ni, Co, Sr, Tl, Pb, W, Th, Zr and Hf. Concentrations of elements V and Ga are similar to those in the UCC (Fig. 3).

Hami mineralization zone

The concentrations of REEs in turquoises found in the Hami mineralization zone are 3.11–212.33 ppm, and the REE pattern is characterized by a depleted to slightly enriched ratio of light-REE (LREE) to heavy-REE (HREE) (Table 1, Fig. 3). All the turquoise deposits in this region have varying degrees of negative Ce anomalies. Hami turquoises show different multi-element patterns normalized to the UCC from those in Qinling mineralization zone. They mostly show an enrichment in Li, V, Cr, Mo, In, Zn and U, and depleted in Ni, Co, Tl, Pb, W, Th, Zr, Hf, compared to the UCC. The concentrations of Sr, Ba Cd and Ga vary widely within Hami turquoise deposits (Fig. 3).

Maanshan mineralization zone

The REE contents of the turquoise deposits in the Maanshan mineralization zone are mostly lower than that of the UCC. They show depleted to enriched LREE concentration patterns, with $(La/Yb)_{UC}$ ratios ranging from 0.17 to 17.74 and slightly negative Ce anomalies [$(Ce/Ce^*)_{UC} = 0.87–0.99$] (Table 1, Fig. 3). Most of the trace elements in these turquoises are lower than those of both the UCC and the turquoise deposits of the Qinling and Hami mineralization zones. Only the presence of Co, In and Zn are enriched in comparison to the UCC (Fig. 3).

Discussion

Previous studies have demonstrated that paleo-redox conditions during deposition of rocks can be appraised from redox-sensitive trace elements, such as V, Ni, Mo, U, Cr, Co and Mn [24–26], and paleo-salinity can be evaluated by Sr, Ba, B, Ga, etc. [27–29]. Upper crust-normalized spider diagrams show that turquoises in China have obviously differences in Ni, Co, Sr and Ba. The Xichuan turquoise deposits have negative Co but no Sr or Ba anomalies, the Bijiashan turquoise deposits in the Maanshan mineralization zone show negative Ni, Sr and abnormal Co, Ba anomalies. The other turquoise deposits were founds to be depleted in Ni, Co, Sr and Ba (Figs. 2, 3). However, the Sr concentration of turquoise deposits in the Hami mineralization zone is higher than Ba concentration (Fig. 3), while the turquoise deposits in the Qinling mineralization zone have more Ba than Sr (Figs. 2, 3). The variation of Ni/Co ratios are usually utilized to estimate the oxidation state of the sedimentation environment, with higher Ni/Co ratios relating to more anoxic conditions [30]. Turquoise deposits in the Maanshan mineralization zone has the lowest Ni/Co ratio. Most of turquoises in the Qinling mineralization zone have similar Ni/Co ratios to those in the Hami mineralization zone, but the Xichuan turquoise deposits show a higher Ni/Co ratio (Fig. 4a). Sr and Ba display contrasting geochemical behaviors in various sedimentation environments, their ratio is sensitive to the salinity of the water [31, 32]. Generally, a high Sr/Ba ratio indicates high salinity, and a low Sr/Ba ratio reflects low salinity [33, 34]. The turquoise deposits in the Hami mineralization zone show the highest Sr/Ba ratios. Meanwhile, although the turquoise deposits in the Qinling and Maanshan mineralization zones have similar Sr/Ba ratios, the Xichuan turquoise deposits show slightly a higher Sr/Ba ratio than the other turquoise deposits in the Qinling mineralization zone (Fig. 4a). Based on this it is apparent that comparison of the presence of redox-sensitive and salinity-sensitive trace elements such as Ni, Co, Sr and Ba are effective in distinguishing the turquoises from these three different mineralization zones. Moreover, Xichuan turquoises could also be distinguished from other turquoise deposits in the Qinling mineralization zone.

In order to further distinguish between turquoise deposits from the Qinling and Hami mineralization zones, it was necessary to examine other sedimentary environment sensitive trace elements. The V/Mo and Ce/Ce^* ratios are also utilized to interpret the redox conditions, with lower V/Mo and higher Ce/Ce^* ratios relating to more anoxic conditions [35–37]. In the Qinling mineralization zone, the Lamadong and Yueertan turquoise deposits mostly have higher V/Mo ratios than the Luonan, Baihe and Yungaisi turquoise deposits, and the Ce/Ce^* ratio of Lamadong turquoise is lower (Fig. 4b). Additionally, the Yueertan, Baihe, Yungaisi and Luonan turquoise deposits are enriched in Ga to varying degrees, compared to Tl (Figs. 2, 3). Ga enrichment is usually caused by redox conditions [38, 39]. However, they also show different Li/Ba ratios, relating to the migration of sediment [40]. In comparing Li/Ba vs. Tl/Ga (Fig. 4c) it can be seen that the Yueertan turquoise deposits have the lowest Tl/Ga ratio, while the Luonan turquoise deposits have the highest Li/Ba ratio. The Yungaisi and Baihe

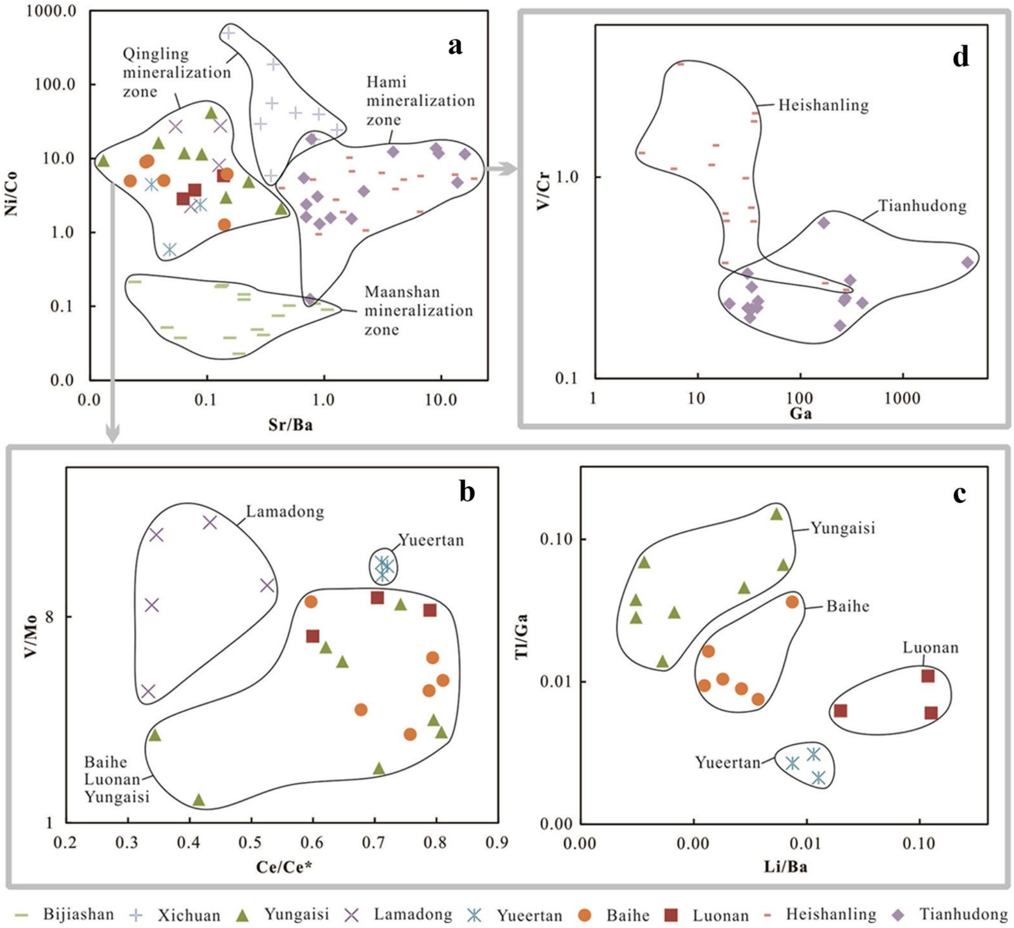

Fig. 4 Scatter graphs showing (**a**) Sr/Ba versus Ni/Co diagram for all turquoise deposits in dataset; (**b**, **c**) Ce/Ce* versus V/Mo for all turquoise deposits in dataset; (**b**) Li/Ba versus Tl/Ga for all turquoise deposits in dataset; (**c**) Li/Ba versus Tl/Ga of turquoises deposits in the Qinling mineralization zone; (**d**) Ga versus V/Cr for turquoises in the Hami mineralization zone

turquoise deposits show similar Li/Ba ratios, but the Tl/Ga ratio of the Yungaisi turquoise deposits is higher than that of the Baihe turquoise deposits.

The Heishanling and Tianhudong turquoise deposits in the Hami mineralization zone both have different Ga concentrations. Ga concentration is sensitive to the salinity of the water [27]. The higher Ga concentration of the Tianhudong turquoise deposits probably indicates that they were formed in a lower salinity environment (Fig. 4d). In addition, the Tianhudong turquoise deposits are depleted in V, compared to Cr, but most of the Heishanling turquoise deposits have no V anomalies (Fig. 3). The V/Cr ratio of the Heishanling turquoise deposits is higher than that of the Tianhudong turquoise depsoits (Fig. 4d), probably reflecting a more anoxic condition [30, 36, 37].

At the same time, we noticed that the turquoise mineral materials in these 9 turquoise deposits cannot be completely distinguished using the elements and their ratios mentioned above. The Sr/Ba and Ni/Co ratios of the Xichuan turquoise deposits have a certain overlap with those of the Hami mineralization zone(Fig. 4a), while the V/Cr ratio and Ga concentration of the Heishanling and Tianhudong turquoise deposits have a certain overlap(Fig. 4d). In addition, only turquoise from 9 turquoise deposits was studied in this article, and the number of turquoise samples from each mine site was limited. Therefore, there is a certain uncertainty in using sensitive elements of sedimentary environment and their ratios to distinguish turquoise from different origins in China, and further in-depth research is needed.

Conclusions and suggestions for future study

With these results, we suggest that sedimentary environment sensitive elements (Ni, Co, Sr, Ba, V, Mo, Ce, Tl, Ga, Li and Cr) and their ratios are effective discriminators of turquoise sources in China, and trace element signatures of turquoise sources vary geographically based on differences in their geologic settings. This sedimentary environment sensitive element based study permits an approach to archaeological questions of turquoise provenance in China.

Future research will be needed to confirm or expand upon sensitive element types and the range of their concentrations and ratios associated with turquoise from each source area that we have characterized. Additional measurements will be especially important for sources from which we currently only have limited samples and those in which we have observed widely variable element concentrations. It will also be necessary to collect trace element data on further turquoise sources that were not included in this study.

Acknowledgements
Thanks to Francesca Monteith for her guidance on the language of this article.

Author contributions
YX raised funding and wrote the manuscript. YL designed the experiments and performed the analysis of the data used in the manuscript. CY and LY collected samples and performed LA-ICP-MS analysis on the samples. YW provided advice on the study, provided the experimental equipment and revised the manuscript. All authors read and approved the final manuscript.

Funding
This study was funded by the Open Fund of Key Laboratory of Cultural Heritage Research and Protection Technology, Ministry of Education, Northwest University (Grant No. GXYDFA2018XBD007) and National Fund of Nature Science of China (Grant No. 51704241). The research was also partial funded by Humanities, Social Sciences Fund of the Ministry of Education (Grant No. 17YJC780007) and the Natural Science Basis Research Plan in Shaanxi Province of China (2022JQ-287).

Availability of data and materials
The datasets used and analysed during the current study are available from the corresponding author on reasonable request.

Declarations

Competing interests
The authors declare that they have no competing interest in this work.

Received: 13 July 2023 Accepted: 1 November 2023

References
1. Henan Provincial Institute of Cultural Heritage and Archaeology. Wuyang Jiahu (I) (in Chinese). Beijing: Science Press; 1999.
2. Qin XL. Turquoise ornaments and inlay technology in ancient China. Asian Perspect. 2016;55(2):208–39.
3. Smolarski, Philippe. The history of turquoise and mining in China. 2021. https://www.researchgate.net/publication/355466942.
4. Foord EE, Taggart JE. A reexamination of the turquoise group: the mineral aheylite, planerite (redefined), turquoise and coeruleolactite. Mineral Mag. 1998;62(1):93–111.
5. Thibodeau AM, Killick DJ, Hedquist SL, Chesley JT, Ruiz J. Isotopic evidence for the provenance of turquoise in the southwestern United States. GSA Bull. 2015;127(11–12):1617–31.
6. Thibodeau AM, Leonardo LL, Killick DJ, Berdan FF, Joaquin R. Was aztec and mixtec turquoise mined in the American Southwest. Sci Adv. 2018;4(6):9370.
7. Hedquist SL, Thibodeau AM, Welch JR, et al. Canyon creek revisited: new investigations of a late prehispanic turquoise mine, Arizona, USA. J Archaeol Sci. 2017;87:44–58.
8. Hull SK, Fayek M, Mathien FJ, et al. A new approach to determining the geological provenance of turquoise artifacts using hydrogen and copper stable isotopes. J Archaeol Sci. 2008;35(5):1355–69.
9. Hull SK, Fayek M. Cracking the code of pre-Columbian turquoise trade networks and procurement strategies. 2012. https://www.researchgate.net/profile/Sharon-Hull.
10. Hull SK, Fayek M, Maxwell T, Antillon RC. Chasing beauty: evidence for Southwestern U.S. Turquoise in Mexico. 2013. https://www.researchgate.net/profile/Sharon-Hull.
11. Ye X, Ren J, Xu H, Chen G, Zhao H. A preliminary study on geological provenance of turquoise artifacts from Erlitou site (in Chinese). Quater Sci. 2014;34(1):212–23.
12. Xian Y, Fan J, Li X, Li Y, Zhou X, Gao Z, Wu M. Research on the source characteristics of Luonan turquoise by using strontium isotopic method (in Chinese). Northwest Geol. 2018;51(2):108–15.
13. Bruggencate RET, Fayek M, Brownlee K, Milne SB, Hamilton S. A combined visual-geochemical approach to establishing provenance for pegmatite quartz artifacts. J Archaeol Sci. 2013;40(6):2702–12.
14. Wang R, Wang C, Feng M, Pan W. The provenance research of turquoise by trace elements analysis (in Chinese). Cult Relics Central China. 2007;2:101–6.
15. Qin SX, Xu YY, Li HM, Li SX, Xi QF. Turquoise mine and artefact correlation for some Bronze age archaeological sites in Hubei province, China. Archaeometry. 2015;57(5):788–802.
16. Xian Y, Li Y, Tan Y, Wang W, Yang Q, Cui J. Application of LA-ICP-AES to distinguish the different turquoise mines (in Chinese). Spectrosc Spectr Anal. 2016;36(10):3313–9.
17. Tu H. Geological characteristics of turquoise ore in the areas adjacent to Shaanxi and Hubei provinces (in Chinese). Geol Shaanxi. 1996;14(2):59–64.
18. Chen J, Zheng Y, Gao JB, Wang JL, Pang JC. The establishment of Cambrian stratigrahy and prospecting significance in the horseshoe hill region of Beishan area Xinjiang (in Chinese). Xinjiang Geol. 2009;27(3):222–7.
19. Li YX, Tan YC, Jia Q, et al. Preliminary investigation of two ancient turquoise mine sites in Hami, Xinjiang (in Chinese). Archaeol Cult Relics. 2019;06:22–7.
20. Yang XY, Zheng YF, Yang XM, Liu XH, Wang K. Mineralogical and geochemical studies on the different types of turquoise from Maanshan area, East China. Neues Jahrb Mineral Monatsh. 2003;3:97–112.
21. Taghipour B, Mackizadeh MA. The origin of the tourmaline-turquoise association hosted in hydrothermally altered rocks of the Kuh-Zar Cu-Au-turquoise deposit, Damghan, Iran. Neues Jahrbuch für Geologie und Paläontologie Abhandlungen. 2014;272(1):61–77.
22. Hull SK. Turquoise exchange and procurement in the Chacoan world. Winnipeg: University of Manitoba; 2012.
23. She LZ, Qin Y, Luo WG, Huang FC, Li TY. Provenance-tracing of Turquoise in Northwest Hubei using rare earth elements (in Chinese). Chin Rare Earths. 2009;30(05):59–62.
24. Morford JL, Emerson S. The geochemistry of redox sensitive trace metals in sediments. Geochim Cosmochim Acta. 1999;63(11):1735–50.
25. Algeo TJ, Maynard JB. Trace-element behavior and redox facies in core shales of Upper Pennsylvanian Kansas-type cyclothems. Chem Geol. 2004;206(3):289–318.
26. Tribovillard N, Algeo TJ, Lyons T, Riboulleau A. Trace metals as paleoredox and paleoproductivity proxies: an update. Chem Geol. 2006;232(1):12–32.
27. Chen Z, Chen Z, Zhang W. Quaternary stratigraphy and trace-element indices of the Yangtze Delta, Eastern China, with special reference to marine transgressions. Quatern Res. 1997;47(2):181–91.
28. Wei W, Algeo TJ. Elemental proxies for paleosalinity analysis of ancient shales and mudrocks. Geochim Cosmochim Acta. 2020;287:341–66.
29. Wei W, Algeo TJ, Lu Y, et al. Identifying marine incursions into the Paleogene Bohai Bay Basin lake system in northeastern China[J]. Int J Coal Geol. 2018;200:1–17.
30. Jones B, Manning DAC. Comparison of geochemical indices used for the interpretation of palaeoredox conditions in ancient mudstones. Chem Geol. 1994;111(1):111–29.

31. Cluff RM. Paleoenvironment of the new albany shale group (Devonian-Mississippian) of Illinois. J Sediment Res. 1980;50(3):767–80.
32. Jia J, Liu Z, Bechtel A, Strobl SAI, Sun P. Tectonic and climate control of oil shale deposition in the upper cretaceous Qingshankou formation (Songliao Basin, NE China). Int J Earth Sci. 2013;102(6):1717–34.
33. Wang A, Wang Z, Liu J, et al. The Sr/Ba ratio response to salinity in clastic sediments of the Yangtze River Delta. Chem Geol. 2021;559:119923.
34. Zhang X, Lin C, Zahid MA, et al. Paleosalinity and water body type of eocene Pinghu formation, Xihu depression, East China Sea Basin. J Petrol Sci Eng. 2017;158:469–78.
35. Elderfield H, Greaves MJ. The rare earth elements in seawater. Nature. 1982;296(5854):214–9.
36. Zhou C, Jiang SY. Palaeoceanographic redox environments for the lower Cambrian Hetang Formation in South China: Evidence from pyrite framboids, redox sensitive trace elements, and sponge biota occurrence. Palaeogeogr Palaeoclimatol Palaeoecol. 2009;271(3):279–86.
37. Gallego-Torres D, Martinez-Ruiz F, De Lange GJ, Jimenez-Espejo FJ, Ortega-Huertas M. Trace-elemental derived paleoceanographic and paleoclimatic conditions for Pleistocene Eastern Mediterranean sapropels. Palaeogeogr Palaeoclimatol Palaeoecol. 2010;293(1):76–89.
38. Flegal AR, Sanudo-Wilhelmy S, Fitzwater SE. Particulate thallium fluxes in the northeast pacific. Mar Chem. 1989;28(1):61–75.
39. Qin G, Cao D, Wei Y, et al. Geochemical characteristics of the Permian coals in the Junger-Hebaopian mining district, northeastern Ordos Basin, China: key role of paleopeat-forming environments in Ga-Li-REY enrichment. J Geochem Explor. 2020;213:106494.
40. Song J, Xu Y, Duan L. Geochemical covariation characteristics of Li/Ba and Rb/Sr and their environmental indication in recent hundred years of the Bohai Bay (in Chinese). Mar Sci. 2014;38(1):79–84.
41 Rudnick RL, Gao S. Composition of the continental crust. In: Holland HD, Turekian KK, editors. Oxford: treatise on geochemistry. Amsterdam: Elsevier; 2014.

Publisher's Note